Development of a cost-effective and flexible vibration DAQ system for long-term continuous structural health monitoring

Theanh Nguyen [a,*], Tommy H. T. Chan [a], David P. Thambiratnam [a], Les King [b]

[a] School of Civil Engineering & Built Environment, Science and Engineering Faculty,
Queensland University of Technology, Brisbane, QLD, Australia
[b] Faculty Services, Science and Engineering Faculty,
Queensland University of Technology, Brisbane, QLD, Australia

ABSTRACT

In the structural health monitoring (SHM) field, long-term continuous vibration-based monitoring is becoming increasingly popular as this could keep track of the health status of structures during their service lives. However, implementing such a system is not always feasible due to on-going conflicts between budget constraints and the need of sophisticated systems to monitor real-world structures under their demanding in-service conditions. To address this problem, this paper presents a comprehensive development of a cost-effective and flexible vibration DAQ system for long-term continuous SHM of a newly constructed institutional complex with a special focus on the main building. First, selections of sensor type and sensor positions are scrutinized to overcome adversities such as low-frequency and low-level vibration measurements. In order to economically tackle the sparse measurement problem, a cost-optimized Ethernet-based peripheral DAQ model is first adopted to form the system skeleton. A combination of a high-resolution timing coordination method based on the TCP/IP command communication medium and a periodic system resynchronization strategy is then proposed to synchronize data from multiple distributed DAQ units. The results of both experimental evaluations and experimental-numerical verifications show that the proposed DAQ system in general and the data synchronization solution in particular work well and they can provide a promising cost-effective and flexible alternative for use in real-world SHM projects. Finally, the paper demonstrates simple but effective ways to make use of the developed monitoring system for long-term continuous structural health evaluation as well as to use the instrumented building herein as a multi-purpose benchmark structure for studying not only practical SHM problems but also synchronization related issues.

KEYWORDS: SHM, long-term continuous monitoring, cost-effective, sensor solution, distributed DAQ, data synchronization

1. Introduction

In the structural health monitoring (SHM) field, long-term continuous vibration-based monitoring of civil structures is becoming more popular in recent years. This is owing to the fact that this type of systems will enable to keep track of the genuine health status of real structures under the disturbance of environmental and operational (E&O) factors [1, 2]. As a result, the structural engineering community has seen an increasing number of bridges and buildings around the world equipped with such monitoring systems [1, 3-5]. Nevertheless, implementing such a monitoring system is not always feasible due to the on-going conflicts between budget constraints and the need of sophisticated monitoring systems for real-world monitoring applications [2, 4]. These problems often become

*Corresponding author at: School of Civil Engineering and Built Environment, Queensland University of Technology, GPO Box 2434, Brisbane, QLD 4001, Australia.
Tel.: +61 731380741
E-mail: theanh.nguyen@qut.edu.au (T. Nguyen)

worse when the measurement coverage is large or sparse. This is particularly true for the conventional DAQ system where every sensor needs to be cabled to one single centralized DAQ station leading to massive cost of the cable itself and the installation labor. To overcome these issues, the recent trend in SHM is to use distributed DAQ system platforms in which each system consists of a network of peripheral DAQ units and their sensors [6, 7]. The DAQ units are linked to each other and to the base station via either radio signal (wireless system) or Ethernet cable (Ethernet-based system). Since each local DAQ unit only needs to be in charge of a small group of adjacent sensors, this type of system greatly mitigates the burden of wiring directly from every sensor to the host station and avoids the problem of signal noise induced by lengthy cabling [6]. In this regard, wireless sensor networks especially those belonging to the SHM-oriented platform could be considered as the first promising candidate. This type of sensors can completely eliminate the demand for cabling among units and therefore be more affordable while suffice for even demanding global SHM applications such as modal analysis of real civil structures [8, 9]. However, to date, successful applications reported for this type of systems have mostly been for short-term monitoring projects [8, 10]. The usage of wireless sensor systems for long-term monitoring is still uncertain due to inherent difficulties such as constraints of power supply and bandwidth; and lower reliability of each node and the whole system particularly over long periods of time [2, 4, 11]. On the other hand, the Ethernet-based DAQ systems, though well-known for their reliability and durability, may still be expensive for most of SHM projects especially from the return on investment viewpoint [3, 4]. More reasonable solutions at sensor and DAQ levels would make this type of systems more appealing so that they can be more widely applied on civil infrastructure particularly in permanent monitoring basis to provide higher safety for society.

To address this issue, this paper presents the development of a cost-effective and flexible vibration DAQ system for the purpose of long-term continuous SHM of a newly constructed complex with a special focus on the system components on the main building. The biggest challenges in developing this system are that the budget is tight while the sensors are distantly distributed and the system is operated in challenging ambient vibration conditions. To overcome such difficulties, multi-layer solutions are derived and implemented. At the lowest system level, the most appropriate accelerometers and their optimal positions are first selected so that they could overcome common adversities in ambient vibration monitoring of civil infrastructure such as low-frequency and low-level vibration measurements. A cost-optimized Ethernet-based DAQ model is then selected to form the system skeleton so that each group of nearby measurement channels can be handled by one local DAQ unit within a network. Instead of using costly hardware-based synchronization methods as normally seen in the traditional approach, the synchronization task for the building vibration sensors is left open for possible inexpensive software-based solutions. As one of the first solutions in the proposed direction, a combination of a high-resolution timing coordination method and a system

resynchronization strategy is proposed to synchronize data from multiple distributed DAQ units. To facilitate accurate verifications of the proposed solutions, a detailed numerical model of the building test-bed is constructed and intensive experimental analyses are used to assess the quality of the vibration data acquired by the developed DAQ system. The outcomes of these evaluations as well as subsequent monitoring applications show that the proposed DAQ and data synchronization solutions work very well and the corresponding system can be used to provide useful long-term continuous health evaluation programs for real-world in-service civil structures.

The layout of this paper is as follows. The second section provides an overview of the instrumented complex and its three main monitoring systems as well as the adopted DAQ model. The third section first presents two solutions - one for selection and placement of vibration sensors and the other, as one of the most significant contributions of this research, for data synchronization of multiple DAQ units distributed on the building structure. Also included in the third section is the introduction of a numerical model of the building to assist the sensor solution as well as later verification tasks. Experimental validations and experimental-numerical modal comparisons as well as long-term continuous health evaluation applications are provided in the fourth section before the fifth section summarizes and concludes the research work.

2. Overview of the instrumented complex and monitoring systems

The instrumented complex is the newly-constructed Science and Engineering Centre (SEC) at the Gardens Point campus of Queensland University of Technology (QUT), Australia. Costing around AUD 230 million, this complex has achieved 5-star Green Star rating from the Green Building Council of Australia making it one of the highest rated green buildings in Brisbane City. Besides being a main teaching and research facility, SEC is also notable for its giant digital lab named “the Cube” (www.thecube.qut.edu.au). With a two-story interactive digital learning and display screen and many other digital science spaces, the Cube is dedicated to be a dynamic hub of hands-on scientific exploration for not only the QUT community and the wider public.

In structural details, the SEC complex comprises two 10-level buildings (named Y and P, as seen in Fig. 1) and various functional spaces underneath the atrium connecting these two buildings. As the main building of the complex, P block houses the Cube and is the main site for deployment of three major monitoring systems namely (1) vibration monitoring system; (2) structural monitoring system (mostly on level 1); and (3) subsurface monitoring system (at the basement) (see Fig. 1 for illustration of these three systems). Besides P block, part of the vibration system is also deployed on the reinforced concrete footbridge located in the front corridor linking the main entrances of the two buildings. This is also the deployment location of two acoustic emission (AE) sensors which, due to their proximity, are able to share the DAQ unit with all the footbridge vibration sensors. Whilst accelerometers are the sole sensor type in the vibration system, the structural and subsurface systems

have mostly employed surface (ST350-type) strain transducers, embedded (vibrating wire-type) strain meters and earth pressure cells. Beside the main vibration system, there are two minor vibration monitoring points, also located within the footprint of P block, to monitor a slab underneath a transmission electron microscope at level 6 as well as to measure ground acceleration for seismic monitoring and referencing purposes. Further usage descriptions of these two monitoring points as well as the other sensors of the AE, structural and subsurface systems are beyond the scope of the present paper and may be reported elsewhere in future.

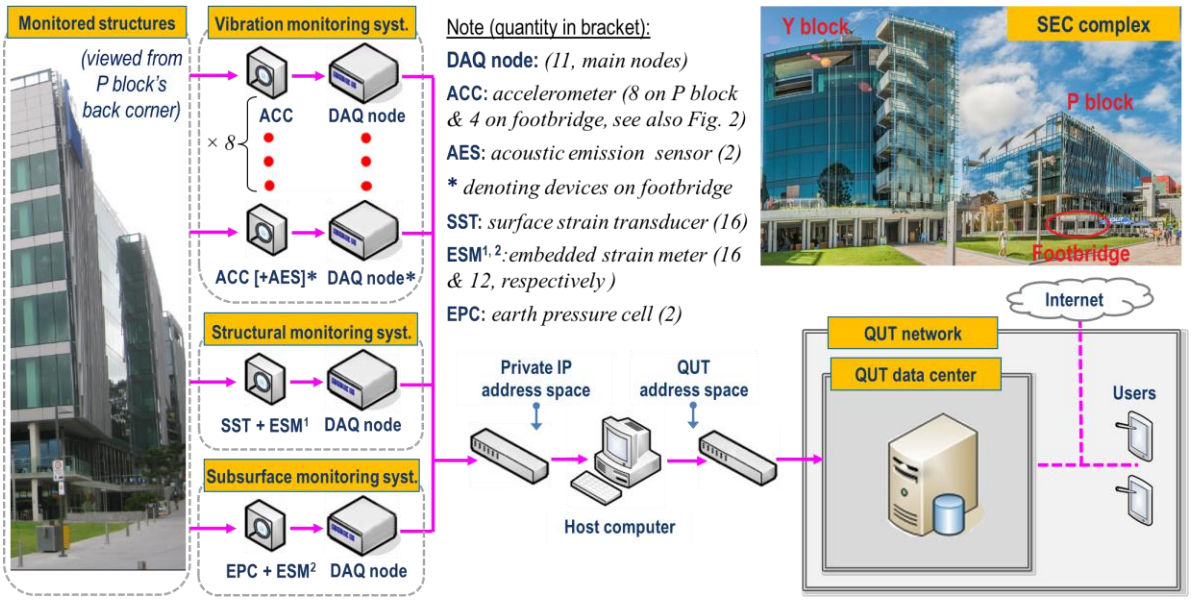

Fig. 1. SEC complex (upper-right) and its three main monitoring systems.

With all the sensors in general and the vibration sensors in particular broadly and distantly located across structures and levels, the distributed DAQ architecture, as illustrated on the left of Fig. 1, is found the most applicable. Well-known for their compact-size, stability and cost-effectiveness, the compact reconfigurable input output (cRIO) platform from National Instruments (www.ni.com/crio) in general and the cost-optimized cRIO-907x series in particular is specially considered as a potential candidate for the DAQ skeleton for all the monitoring systems herein. The finally selected model (cRIO-9074) is one of three models (besides cRIO-9072 and cRIO-9073) of the cRIO-907x series available during the design phase of this project. The cRIO-9074 is more advantageous than the other two models due to its capacity of chassis expansion as this model has another Ethernet port (beside the one exclusively for network connectivity) that can be used for such a purpose. Last but not least, the adoption of the same DAQ model for all systems in this instrumentation project ensures that the tasks of system deployment, programming, operational management and future maintenance can be all simplified.

3. Vibration sensor and data synchronization solutions

3.1. Vibration sensor solution

The first mission in this phase is to select the appropriate accelerometers. As the main target for the system is to be serviceable in ambient vibration context, the main features of the accelerometers such as sensor type, measurement range and sensitivity are considered as the most critical factors among others. First, the capacitive type is selected as this type of accelerometers is more applicable for low-frequency (around 1 Hz for P block, see Fig. 3) and low-level (as small as 1-2 mg) vibration measurements than other types such as piezoelectric sensors [4, 11, 12]. Also to overcome the latter issue, high-sensitivity accelerometers need to be prioritized to reduce the noise impact and to enhance the quality of the recorded data [4, 11, 12]. The low-level vibration measurement issue tends to occur in the case of the two instrumented structures herein. This is because the P block, with a limited height of around 40 m against its typical (upper) floor dimensions of 45 m by 63.5 m, is no doubt a non-slender building. Made up of a 375mm-thick slab and two 500mm-high edge beams, the concrete-type footbridge of 8.5m span herein can be considered as a non-flexible structure. Such building or footbridge structures tend to be marginally excited by ambient excitation and therefore need higher attention in sensor selection to enable their small motions to be properly recorded. Based on the above criteria, the selected sensors are all capacitive micromachined analog accelerometers (from Silicon Designs, Inc.) with a reasonable measurement range (+/- 2g) and high sensitivity for this sensor type (2000mV/g). However, due to budget constraints, only 8 tri-axial and 4 single-axis accelerometers of this type are finally allocated to the main vibration system. The four-channel analog input module (NI-9239) is used to serve as the interface between the accelerometers and the cRIO-9074 chassis providing analog-digital converter (ADC), anti-aliasing filter and peripheral sampling control.

With such a limited number of accelerometers, sensor positioning must be carefully designed to maximize the information captured from both the building and the footbridge. First of all, both of these two structures should have tri-axial sensors so that more types of modes (e.g. in different directions or coupled ones) can be measured. Besides, in planar-type structures such as the footbridge herein, the tri-axial sensors should be placed in the positions that are the most sensitive to the modes that may be undetected by single-axis sensors such as lateral or torsional modes. Toward this goal, the footbridge is first allocated two tri-axial accelerometers to be positioned on middle of the two unsupported edges as shown in Fig. 2 (left). Additionally, two single-axis sensors are placed to measure the vertical motion at a quarters and three-quarters of the span along the longitudinally central line of this footbridge. The motion of the middle point of this central line can be interpolated from motions captured by the two tri-axial sensors based on the assumption of the cross-section moving as a rigid body.

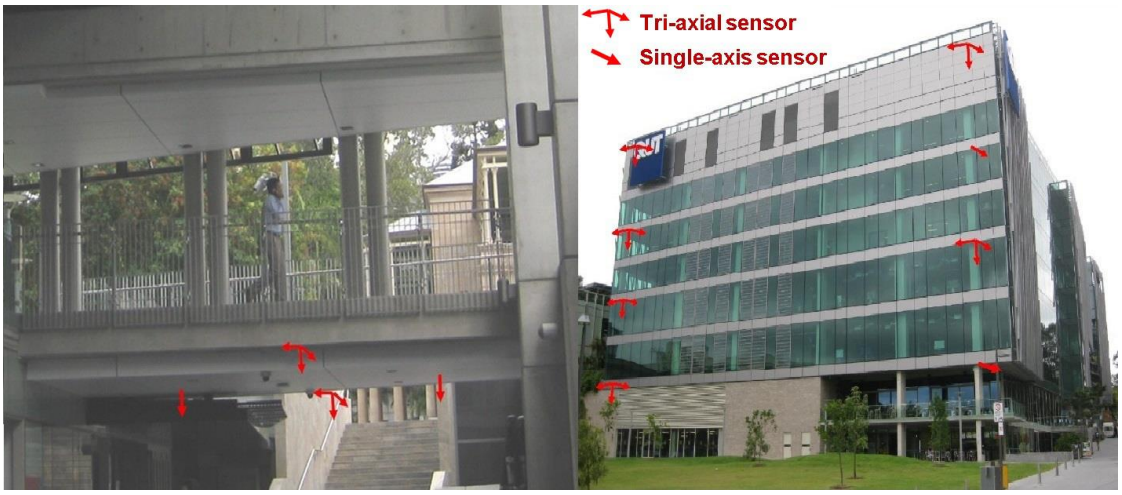

Fig. 2. Sensor position on the footbridge (left) and the building (right).

With regards to the main building, P block has a rather common overall configuration for the building structures of its type with a rather wide semi-underground base consisting of the lowest four levels (see Fig. 7 for illustration of the base). Therefore, it is not too difficult to see that the upper six levels are horizontally more sensitive to ambient excitation and should be the locations for most of the vibration sensors where the signal-to-noise ratio of acceleration data can be enhanced. However, it is still very worthwhile to investigate the dynamic behaviour of the building to verify the fundamental vibration frequency as well as to characterize the vibration modes and floor motions for the purpose of confirming the sensor solution as well as optimizing sensor placement scheme. To do so, a 3D numerical model is constructed using SAP2000 software (version 15.2) and as-built drawings in order to take into account all the structural modifications during the construction phase. The model, as shown in Fig. 3 consists of approximately 1400 frame elements (for beams and columns) and 8000 shell elements (for slabs and shear walls). The numerical modal analysis results show that all of the first five modes are global and can be captured by the sensors placed on 4 out of the 6 upper levels of the building. The results also show that these five global modes range from 0.99 Hz to 4.97 Hz and include modal displacements from either X/Y direction (for translational modes, e.g. mode 1) or both (for torsional modes, e.g. mode 5 as illustrated in Fig. 3). These help to reconfirm the needs of capacity-type accelerometers (for low-frequency measurement) as well as 2D measurement of horizontal vibration responses. The modal animations also show that the rigid body motion theory holds reasonably well for all the upper floors including those that have floor openings. As a result, the horizontal movement of each floor level can be described via two horizontal displacements and one deformation angle [13]. A minimum number of two sensors can be used at two adjacent corners of the floor and one of these two sensors can be in single-axis type. Consequently, four floor levels can be

covered with eight remaining accelerometers leading to the building sensor placement solution as illustrated in Fig. 2 (right). Unmeasured horizontal degrees of freedom for mode shape animation purposes will be interpolated from measured ones.

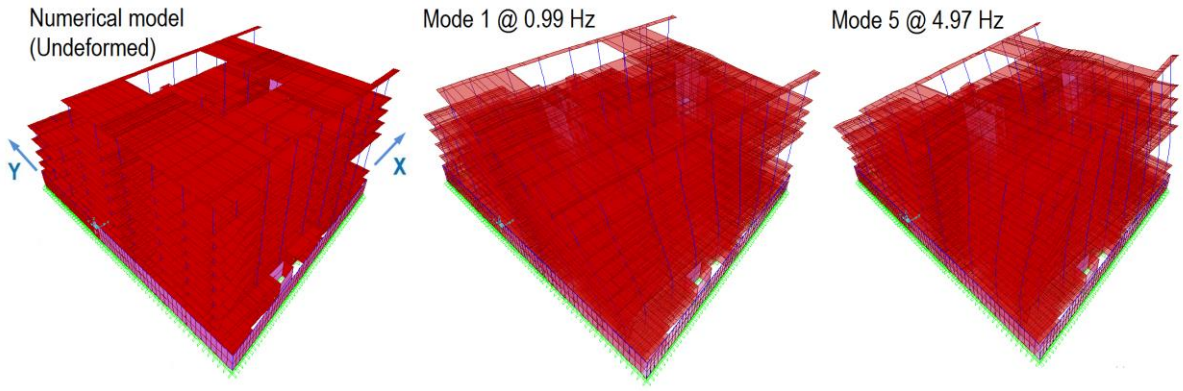

Fig. 3. Numerical model of the building and its two representative modes.

3.2. Data synchronization solution

Being located within proximity of each other, all footbridge sensors only required one DAQ unit to be shared and consequently, these sensors can be precisely synchronized without requiring any additional hardware. This synchronization is realized by sharing the master timebase of any input module with the others in the same chassis. In contrast, as the building vibration sensors are distant from each other, one DAQ node needs to be allocated for each of these sensors to effectively reduce the cable length and enhance the data quality as previously discussed. The remaining issue is how to properly synchronize multiple peripheral DAQ nodes deployed on the building. Large DSE has been shown to negatively affect global vibration-based SHM applications such as modal analysis and associated damage identification [9, 14]. The main hardware-based multi-chassis synchronization option during the system design phase was the use of a digital I/O module in every local DAQ unit in order to form a dedicated synchronization bus. A synchronization trigger pulse can be then generated from the master device and passed to each of the slave devices [15, 16]. However, as this option was prohibitively expensive for the system coverage required herein, the desire for inexpensive and flexible alternatives has triggered the promotion of alternative software-based solutions. The main bases for this direction are first that the main impact of DSE tends to be proportional to the DSE magnitude and the modal frequency value [9, 14, 17]. Second, the frequencies of interest for civil structures where the synchronization task often becomes more problematic are rather low and, for many cases (including the case considered herein), less than 10 Hz. Third, high-resolution timing coordination is feasible with Ethernet connection [15]. It is therefore feasible in system development for such structures to use software-based solutions to achieve a reasonable data synchronization level so that the impact of remaining DSE can be negligible [9]. As one of the first solutions in this

direction, the combination of a customized timing coordination method based on TCP/IP command communication and a periodic system resynchronization strategy will be presented below.

The manner in which a distributed DAQ system operates without a conventional cable-based synchronization bus is as follows. The peripheral DAQ units start their own data sampling process asynchronously based on the sampling command each unit receives from the host computer via TCP/IP communication. Upon receiving this command, the field-programmable gate arrays (FPGA) chip in each unit immediately initiates its analog input module to acquire data based on the internal master timebase of the module. These result in inherent DSE with two main components, namely initial DSE and accumulated DSE, similar to those from wireless sensors [9]. Whilst initial DSE is induced from the difference in the start (sampling) times of multiple DAQ units, accumulated DSE is caused by the inherent difference between multiple local timebases of multiple input modules. Besides controlling the starting times of the individual sampling processes, it is therefore also necessary to resynchronize the system after certain duration of time before the accumulated DSE could become significant to spoil the recorded data.

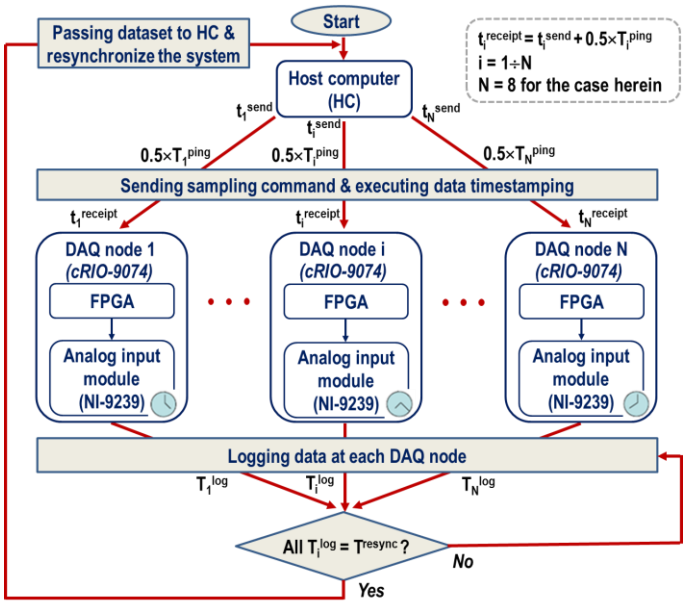

Fig. 4. Flowchart of data synchronization solution.

In order to combat both DSE components, a data synchronization solution is derived as illustrated in Fig. 4 and implemented in the system programming environment (LabVIEW). First, data acquired by each DAQ node is timestamped based on the time the sampling command is supposed to be received at the FPGA chip of the unit. This command delivery time ($t^{receipt}$) is calculated by the time the sampling command (t^{send}) is sent from the host computer plus the duration for the command message to travel from the host computer to the DAQ node. The latter component is actually half of the ping time (T^{ping}, obtained in each ping test) which measures the round-trip travel time of the

command message and can be well estimated by utilizing statistical measures (such as the mean and standard deviation) from a sufficiently large number of ping tests [18]. To achieve high accuracy, the advanced hrPing utility with the time resolution of microseconds is used instead of the basic windows ping utility with limited resolution of milliseconds [19]. This way, the initial DSE has been significantly reduced and has found to be less than 0.1 millisecond (which is equivalent to one fifth of the sampling period); and now mostly due to small fluctuations of the message delivery times at different DAQ nodes. In order to cope with DSE accumulation, the system is programmed to reinitialize the sampling process after a predetermined duration to cut off the growth of DSE. This resynchronization duration (T^{resync}) should at least equate the undisrupted data length required by intended applications such as modal analysis (see the next section for details). Finally, the data streams from different DAQ nodes are aligned with each other by matching their timestamps before other preprocessing tasks such as data decimation can take place.

4. Experimental evaluations

As the main focus of this study, only experimental evaluations of the sensor and data synchronization solutions for the P block building are reported in this section along with a brief experimental–numerical data comparison. Further analyses and model updating studies for the monitored structures will be shortly reported in an upcoming paper of the authors [20].

4.1. General evaluation of the DAQ system

Owing to the delta-sigma modulation of the input module, possible sampling rates can be derived through the formula of 50/*n* kilo samples per second (kS/sec) where the denominator (*n*) can be any integer between 1 and 31 [21]. To cater for convenient choices of decimation factors (in post-processing phases), the primary sampling rate is selected to be 2 kS/sec (i.e. $n = 25$) which is close to the minimum sampling rate value. Next, the data length for an undisrupted acquisition process between two consecutive synchronization points needs to be decided. The commonly-used rule of thumb for this length in ambient modal testing is that it should be around 1000–2000 times the fundamental vibration period [13, 22]. Based on preliminary spectral analyses, the first natural vibration period of P block is shown up to be around 0.9 sec and the undisrupted data acquisition length should therefore be 900–1800 sec. Hence, the resynchronization span is set at 30 minutes and the data streams acquired by multiple DAQ nodes are timestamped and synchronized as previously described. Besides, such a low value of the fundamental frequency (of around 1.1 Hz) has confirmed that the assumption of low-frequency measurement in the instrumentation design phase has become true. A similar confirmation can also be made for the low-level measurement assumption as one thirds of horizontal measurement channels have been found to experience the (peak-to peak) amplitudes of

around 2 mg in normal excitation conditions. For the illustration purpose, Fig. 5 shows a 10-minute time history of such a typical channel in level 8. Overall, the confirmations for both earlier assumptions mean that the adopted accelerometers are appropriate to the vibration characteristics of the intended structure.

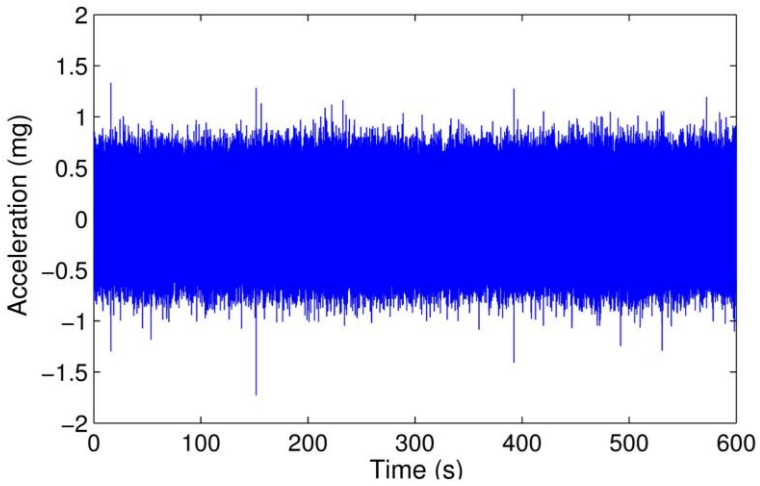

Fig. 5. Typical low-level acceleration time history.

To obtain global vibration characteristics of the P block under ambient excitation conditions, the output-only modal analysis (OMA) approach is used [13]. For the purpose of modal animation and validation, the building is modelled, as illustrated in Fig. 7, at measured levels plus its lowest (ground floor) level that is deemed to have negligible displacement. Amongst different OMA algorithms, data-driven stochastic subspace identification (SSI-data) with the un-weighted principal component estimator is selected as the main OMA technique [13]. This is because this technique has been shown to be as robust against the impact of initial DSE as the well-known frequency domain decomposition (FDD) technique [9]. Further, in comparison with FDD, SSI-data is more advantageous in coping with closely spaced or repeated modes as well as in the implementation of automated modal identification. These can facilitate rapid and accurate OMA which is particularly meaningful for continuous monitoring generally with large quantity of datasets.

Theoretically, SSI-data relies on directly fitting parametric state space models to the measured responses of the structure with model orders being varied up to a user-defined maximum dimension [13, 23]. To reduce computational effort and noise impact associated with the use of a large number of measurement channels, channel projection is often applied [13, 24]. By varying the model order, multiple sets of each modal parameter at a pole are obtained and their deviations are used to examine whether the pole is as stable as to represent a genuine structural mode. This leads to the extensive use of the stabilization diagram in SSI-data to facilitate the task of automated modal identification (see Fig. 6 for illustration). It is also worth noting from this figure that, the background wallpaper of the

diagram consists of the spectral density singular value plots the peaks of which can be used to correlate with the pole locations determined by SSI-data for cross-checking purposes.

Back to this study, via comparing the results of SSI-data of incremental dimensions and projection channels, the most stable range of maximum dimensions is found to be between 120 and 200 whereas that of the projection is from 8 to 10 channels. Hence, the maximum state space dimension of 160 and the projection of 9 channels are selected as the common SSI-data configuration for all vibration datasets of the P block used in this paper. Using this SSI-data configuration, a total of first seven modes can be estimated via the stabilization diagram and validated using mode shape animation as typically illustrated in Fig. 6 and Fig. 7, respectively. Further details of the estimated modes are provided in Table 1 (along with the corresponding frequency values predicted by the numerical model for the purpose of comparison). Note that the experimental values of frequencies and damping ratios in this table are the mean values obtained from a number of datasets which are mainly for use for statistical assessment of synchronization solutions in the next section. Of the seven modes, most are reasonably well excited (i.e. corresponding well to the spectral peaks) with two of them (i.e. modes 2 and 3) being rather closely spaced. In addition, the most weakly-excited one (mode 6) though not always present can still be identified in a certain number of datasets. Such capacities and the achievement of clear mode shape animation views (Fig. 7) for all the seven modes can be attributed for the suitability of not only the sensors and their positions but also the combined synchronization solution in general and the system resynchronization strategy in particular. With regards to experimental–numerical modal comparison, the third column of Table 1 shows a satisfactory agreement between modal frequencies estimated by SSI-data and those predicted by the numerical model (with excellent results for the first four modes) and this can be seen as an additional evidence for the reliability of the vibration DAQ system that has been developed. For external correlation purposes, it is worth comparing the OMA results of the P block herein with similar cases in literature. Toward this point, the two 15-story buildings to be cited are an office building in Japan and the well-known Heritage Court Tower (HTC) in Canada which has been considered as a benchmark structure for ambient vibration testing [25, 26]. By using popular OMA techniques such as FDD or SSI-data, 9 modes from the first building were identified whilst this figure for the HTC building was from 9 to 11 depending on the OMA technique in use. Since the P block has only 10 stories with a high percentage of base levels (35% total height vs. around 25% of the HTC building case), the number of estimated modes (i.e. 6–7) for this building can be seen as to be well reasonable against both quoted reference results.

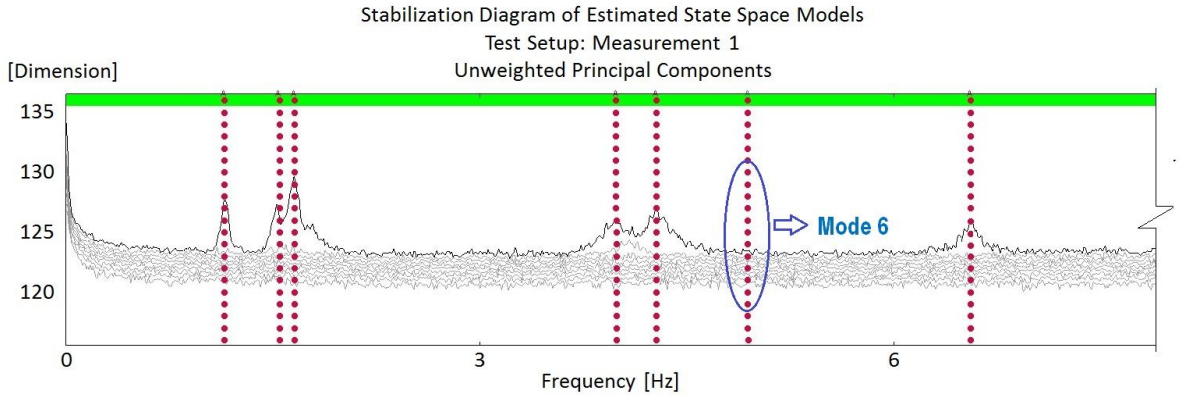

Fig. 6. A typical SSI-data stabilization diagram for OMA of the building.

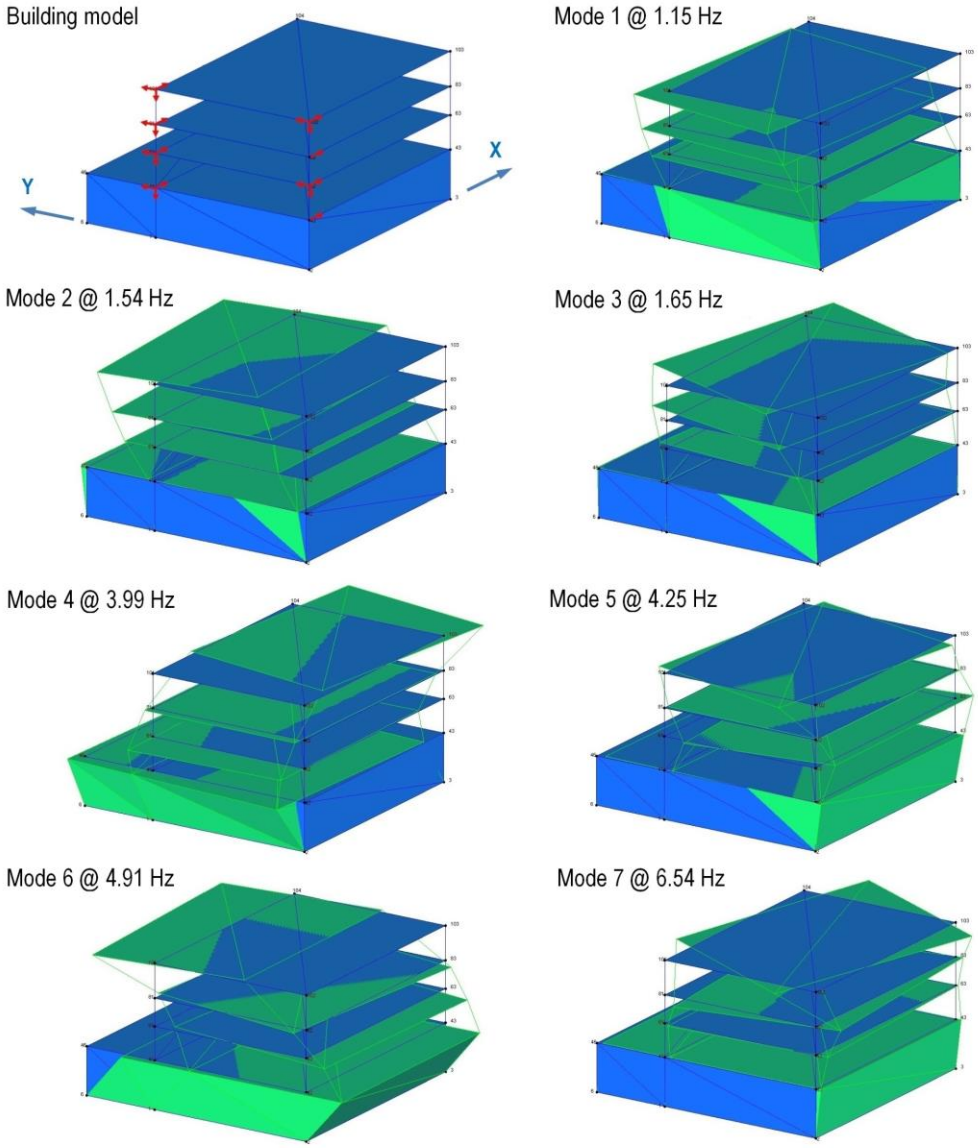

Fig. 7. Building model and typical animation views of seven estimated modes.

Table 1**.** Features of seven estimated modes

Mode no.	Description of modes	Frequency (Hz)	Damping ratio (%)
1	1st translational – X direction	1.15 [0.99]	2.03
2	1st translational – Y direction	1.54 [1.45]	3.59
3	1st torsional	1.65 [1.68]	1.88
4	2nd translational – X direction	3.99 [3.68]	1.98
5	2nd torsional	4.25 [4.97]	2.08
6	2nd translational – Y direction	4.91 [5.60]	5.47
7	3rd torsional	6.54 [8.78]	2.85

(Numerical frequency values provided in square brackets for comparison)

4.2. Statistical evaluation of the data synchronization solution

To evaluate the actual efficacy of the synchronization solution for long-term purposes, repetition checks need to be carried out on multiple datasets to examine the impact of remaining initial DSE that is random in its nature. Since mode shapes have been shown to be significantly more sensitive than frequencies and damping ratios with respect to initial DSE in prior studies [9, 27], it is necessary to assess the impact of initial DSE on the former parameter. The most common method for this is to track changes of modal assurance criterion (MAC) of pairs of mode shape datasets recorded upon different synchronization spans. The challenge for this type of assessment on real structures is that the modal parameters in general and mode shapes in particular are influenced not only by special DAQ uncertainties such as DSE herein but also from common E&O factors such as temperature, wind conditions or human-induced activities. The impact of the latter factors especially temperature has been considered as one of the most significant obstacles against the success of SHM in practice for the purpose of detecting critical changes such as structural damage [2]. To overcome this problem, a daisy chain data selection scheme is derived in this study for computation of MAC data for the aforementioned tracking purpose. To do so, MAC values are strictly calculated from any (two) consecutive datasets in rather uniform E&O conditions. Such selections of data and E&O conditions are to ensure that the time and meteorological spans are so short that the paired datasets are deemed to be subjected to similar E&O influences. Any unusual shift in MAC values could therefore be attributed to the initial DSE.

Applying the above data selection scheme, 50 MAC vectors can be calculated from a total number of 64 reasonable datasets obtained in various days during the system development phase in late 2013. As it is occasionally under-excited during the testing days, mode 6 is excluded from this assessment. Fig. 8 shows the distribution of MAC data for the remaining six (regularly-excited) modes in box-plot, a useful graphical tool for presenting robust statistics [9]. There are a few outliers (maximum 3 out of 50 observations) at some modes but this has no significant impact on the overall result. In fact, one can clearly see that most of the mode-shape sets are in excellent agreement (with each other) with

their MAC values above 0.95 and narrow (statistical) dispersion of around 0.02 or less. The lower figures of MAC at modes 2 or 7 can be attributed to the nature of these two modes i.e. being more damped than the other modes. In contrast, the highest agreement at mode 3 is mainly due to the fact that this is the least damped mode in the detected range. These are reflected via the magnitudes of the damping ratios in Table 1. Nevertheless, such overall high and stable MAC values have proved that the remaining initial DSE is insignificant and the proposed synchronization solution has worked very well.

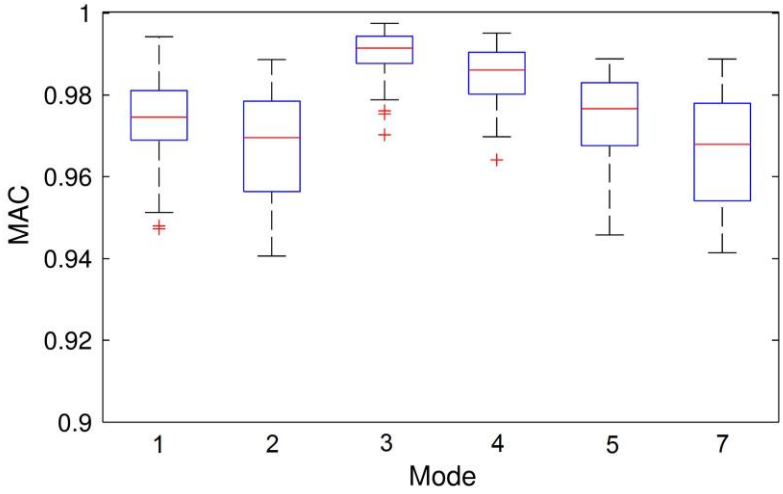

Fig. 8. Statistics of mode shape agreement across multiple datasets

4.3. Continuous structural health evaluation

Previous statistical evaluation has shown that the vibration DAQ system can operate stably and provide useful and reliable vibration data for the long-term monitoring purpose. This would lead to the establishment of representative databases for every definite period of time (e.g. annually) during the structural service life to enable continuous (or at least frequent) evaluation of structural health. In order to deal with the inherent impact of E&O factors, the evaluation problem should be formulated in the pattern recognition framework by means of machine learning algorithms [2]. The use of such an algorithm is to "learn" the underlying trends (caused by E&O factors) present in the training data so that these trends can be separated from the symptom of any potential structural anomaly or novelty (such as damage) present in the testing data. The consequence of this is that the testing result can accurately inform whether the structure has still been in its normal state or not. For illustration purposes, two commonly-used unsupervised learning algorithms, that is, based on Mahalanobis squared distance (MSD) and auto-associative neural network (AANN) are employed in this section. While MSD-based algorithm obtains the knowledge of E&O impact trends mainly through the inclusion of the sample covariance matrix in its computational structure (Appendix A), AANN mainly does this at the bottleneck layer where the trends induced by E&O factors are forced to be prevailing

(Appendix B). The training data used in this section is the frequency data corresponding to the six frequently-excited modes of the 64 aforementioned datasets. Testing data is from 36 datasets collected more recently (in early 2014). The confidence level used for both learning algorithms is set at a commonly-used level of 99 % while a simple AANN architecture is used with the number of nodes at both outer hidden (i.e. mapping and demapping) layers equating to the number of feature variables. At the bottleneck layer, two hidden nodes are used as they are assumed to represent two most dominant E&O factors namely temperature and structural mass [2]. As P block is a main institutional building for teaching and working purposes, the change of the latter factor is supposed to be due to the occupants of this block entering or vacating the building.

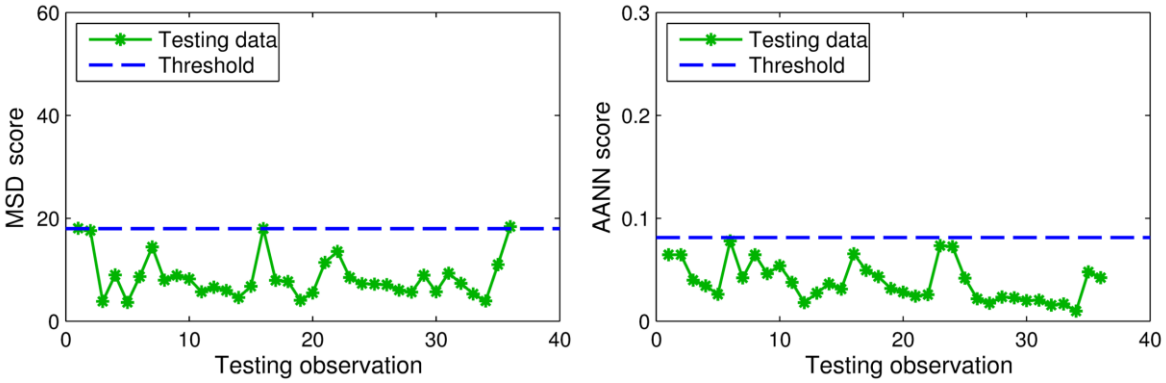

Fig. 9. Novelty detection results: MSD-based (left) and AANN-based (right).

Fig. 9 shows the monitoring results in the form of novelty detection by MSD-based and AANN-based learning algorithms. All AANN scores and almost all of MSD scores lie below the threshold meaning that all the testing observations are likely to be under normal conditions. This can be confirmed by the good agreement between the magnitudes of training and testing data as reflected by their box-plots in Fig. 10. A few extreme MSD scores (slightly larger than the threshold) might be related to the problem of insufficient multinormality in the training dataset as this set has had rather limited (i.e. 64) observations at the current stage. Such a problem has been shown to be able to cause unstable MSD computational outcome [28]. While this problem tends to be overcome in later monitoring stages when more measured data is provided by the sensing system, one possible immediate solution is the use of the controlled Monte Carlo data generation scheme to enhance the training data multinormality degree and therefore robust MSD computation [29]. This issue will be further addressed in the future work of the present authors.

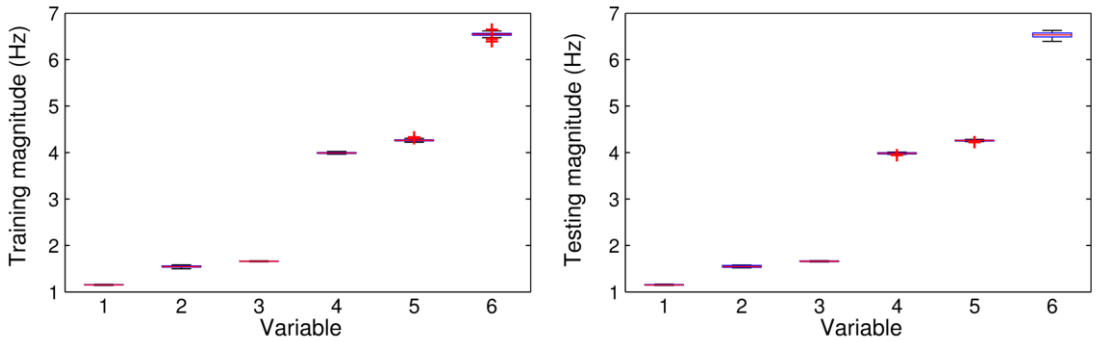

Fig. 10. Box-plots of training data (left) and testing data (right).

5. Summary and conclusion

This paper has presented the detailed development of a cost-effective and flexible vibration DAQ system for long-term continuous SHM of a newly constructed complex in general and its main building in particular. To overcome the challenges of the monitoring conditions and budget constraint, vibration sensors with the most appropriate features have first been selected and their positions have then been optimized so that they can function well under practical difficulties including low-frequency and low-level vibration measurements. To tackle the sparse measurement problem, the distributed DAQ architecture has been adopted and economically realized by a cost-optimized peripheral DAQ model. In search of inexpensive and more flexible alternatives, the software-based signal synchronization approach has been fostered and a novel data synchronization method has been realized by means of high-resolution timing coordination and periodic system resynchronization both enforced from the host level via TCP/IP communication medium. By applying this solution, the initial DSE of the system has been well reduced from uncontrolled levels to be very marginal whereas the accumulated DSE can be effectively kept at minimum. The results of both experimental evaluations as well as experimental-numerical comparisons show that the sensor, peripheral DAQ and data synchronization solutions have worked very well and they can provide a promising alternative for use in the SHM projects with budget constraints and/or sparse measurement coverage where conventional hardware-based synchronization may be too costly. Using the above solutions, the developed DAQ system is shown to be able to provide quality feature databases which can combat the impact of practical E&O factors and establish useful continuous health evaluation processes for real-world civil infrastructure. Using such an open data synchronization scheme, the instrumented building herein can be used as a multi-purpose benchmark structure for vibration-based SHM problems in general and for studying signal synchronization issues in particular. For upcoming future work, building vibration data will be continuously collected and analyzed under different E&O conditions to construct representative databases for tracking the health status of the building or its deterioration process. Other potential synchronization methods can be rapidly applied to examine their efficacy while

multiple classes of data with different levels of DSE can be generated (by relaxing the synchronization process) for synchronization related studies.

Acknowledgements

The first author gratefully appreciates the financial support for his research from the Vietnam Government, Queensland University of Technology (QUT) and QUT School of Civil Engineering and Built Environment. Valuable assistances from Mr. Jonathan James in the system development and implementation phases and from the high performance computing (HPC) supporting team at QUT for data storage issues are also acknowledged with thanks.

Appendix A. MSD-based learning for novelty detection

Suppose that the training dataset has *p* variables and a sufficient multivariate normal (multinormal) distribution. This dataset can therefore be represented by its sample mean vector ($\bar{x}$) and sample covariance matrix (S). By means of MSD technique, each *p*-variate observation (x_i) in either training or testing phases can be transformed into a scalar in the form of distance (or novelty) measure as follows.

$$d_i = (x_i - \bar{x})^T \mathrm{S}^{-1} (x_i - \bar{x}) \qquad (A.1)$$

After computing all training distances, the assumption of a multinormal distribution again allows the estimation of the novelty threshold from the basis of chi-square distribution for the training distances [2]. It is because under such an assumption, one can specify a statistical threshold based on a distribution quantile or a confidence level [2, 28]. In the testing phase, whenever a new feature observation of the structure is recorded, its corresponding distance can then be used to compare against the threshold to determine whether it corresponds to a normal condition or a novelty (such as a damaged state in the SHM context). In spite of being selective in multinormality degree of the input data, MSD-based learning algorithm is well-known for its architectural simplicity and computational efficiency which are advantageous for dealing with large volume of data [28].

Appendix B. AANN-based learning for novelty detection

AANN is a multilayer feed-forward perceptron network which is trained to produce, at the output layer, the patterns that are presented at the input layer [2, 5]. The network contains three hidden layers: the mapping layer, the bottleneck layer and the demapping layer. The mapping and demapping layers consist of neurons with hyperbolic tangent sigmoid transfer functions while the bottleneck and output layers are formed by linear neurons. Typically, both mapping and demapping layers often use the same number of nodes while the bottleneck layer uses fewer nodes so that this special layer can

discard trivial variations and extract the predominant trends such as those induced by E&O factors. Also because of this, the number of hidden nodes at the bottleneck layer is often selected in order to represent such prevalent trends in the data.

Again, suppose the training dataset has p variables, after the network is trained, each p-variate input observation (x_i) in either training or testing phases is passed into the trained network to yield an (p-variate) observation ($\hat{x}_i$) at the network output layer. The corresponding observation of the novelty index in form of the Euclidean distance can therefore be as follows [2].

$$d_i = \left\| x_i - \hat{x}_i \right\| \qquad (B.1)$$

The tasks of threshold determination (based on confidence level) and novelty detection of AANN-based algorithm are then similar to those of MSD-based algorithm (Appendix A). Advantages of AANN-based algorithm include the capacities of dealing with data that may not have a multinormal distribution and recognizing nonlinear underlying trends. However, AANN-based algorithm has more complicated architecture than the MSD-based counterpart and therefore generally requires some user judgment and costs more computational effort in training and testing processes.

References

[1] J.M. Ko, Y.Q. Ni, Technology developments in structural health monitoring of large-scale bridges, Engineering Structures, 27 (2005) 1715-1725.

[2] C.R. Farrar, K. Worden, Structural health monitoring: a machine learning perspective, Wiley, Chichester, West Sussex, 2013.

[3] F. Ansari, Sensing Issues in Civil Structural Health Monitoring, Springer, Dordrecht, The Netherlands, 2005.

[4] V.M. Karbhari, F. Ansari, Structural health monitoring of civil infrastructure systems, Woodhead Publishing, Cambridge, UK, 2009.

[5] T.H.T. Chan, K.Y. Wong, Z.X. Li, Y.Q. Ni, Structural Health Monitoring for Long Span Bridges - Hong Kong Experience & Continuing onto Australia, in: T.H.T. Chan, D.P. Thambiratnam (Eds.) Chapter 1 in Structural Health Monitoring in Australia, Nova Science Publishers, Inc., New York, 2010.

[6] A.E. Aktan, F.N. Catbas, K.A. Grimmelsman, M. Pervizpour, Development of a Model Health Monitoring Guide for Major Bridges, Drexel Intelligent Infrastructure and Transportation Safety Institute, 2002.

[7] H. Van Der Auweraer, B. Peeters, Sensors and systems for structural health monitoring, Journal of Structural Control, 10 (2003) 117-125.

[8] J.A. Rice, B.F. Spencer, Flexible smart sensor framework for autonomous full-scale structural health monitoring, University of Illinois at Urbana-Champaign, Illinois, USA, 2009.

[9] T. Nguyen, T.H.T. Chan, D.P. Thambiratnam, Effects of wireless sensor network uncertainties on output-only modal-based damage identification, Australian Journal of Structural Engineering, 15 (2014) 15-25.

[10] S. Cho, H. Jo, S. Jang, J. Park, H.J. Jung, C.B. Yun, B. Spencer, J.W. Seo, Structural health monitoring of a cable-stayed bridge using wireless smart sensor technology: data analyses, Smart Structures and Systems, 6 (2010) 461-480.

[11] Y.-L. Xu, Y. Xia, Structural health monitoring of long span suspension bridges, Spon Press, New York, 2012.

[12] H. Jo, S.-H. Sim, T. Nagayama, B.F. Spencer, Development and Application of High-Sensitivity Wireless Smart Sensors for Decentralized Stochastic Modal Identification, Journal of Engineering Mechanics, 138 (2012) 683-694.

[13] Structural Vibration Solutions A/S, ARTeMIS Extractor, Release 5.3, User's Manual, Structural Vibration Solutions A/S, Aalborg East, Denmark, 2011.

[14] V. Krishnamurthy, K. Fowler, E. Sazonov, The effect of time synchronization of wireless sensors on the modal analysis of structures, Smart Materials and Structures, 17 (2008) 1-13 (18).

[15] J. Semancik, Ethernet-based instrumentation for ATE, Proceedings of the IEEE AUTOTESTCON 2004, IEEE, San Antonio, TX, USA, 2004, pp. 316-320.

[16] National Instruments, Synchronizing multiple CompactRIO chassis; 2012 (accessed December 2013). Available at (http://www.ni.com/white-paper/4217/en/).

[17] T. Nguyen, T.H.T. Chan, D.P. Thambiratnam, Effects of wireless sensor network uncertainties on output-only modal analysis employing merged data of multiple tests, Advances in Structural Engineering, 17 (2014) 319-329.

[18] Wikipedia contributors, Ping (networking utility); 2001 (accessed December 2013). Available at (http://en.wikipedia.org/wiki/Ping_%28networking_utility%29)

[19] cFos Software GmbH, Ping Utility hrPING v5.06; 2013 (accessed December 2013). Available at (http://www.cfos.de/en/ping/ping.htm).

[20] K.A.T.L. Kodikara, T.H.T. Chan, T. Nguyen, D.P. Thambiratnam, Model updating of real structures with ambient vibration data, (Fully accepted for publication on) Proceedings of the 7th International Conference on Structural Health Monitoring of Intelligent Infrastructure (SHMII) Politecnico di Torino, Torino, Italy, 2015.

[21] National Instruments, NI 9229/9239 Operating instructions and specifications; 2012 (accessed December 2013). Available at (http://www.ni.com/pdf/products/us/922939ds.pdf).

[22] R. Cantieni, Experimental methods used in system identification of civil engineering structures, Proceedings of the 1st International Operational Modal Analysis Conference, Copenhagen, Denmark, 2005, pp. 249–260.

[23] P.V. Overschee, B.D. Moor, Subspace Identification for the Linear Systems: Theory–Implementation-Applications, Kluwer Academic Publishers, Dordrecht, The Netherlands, 1996.
[24] H. Herlufsen, P. Andersen, S. Gade, N. Møller, Identification Techniques for Operational Modal Analysis–An Overview and Practical Experiences, Proceedings of the 1st International Operational Modal Analysis Conference, Copenhagen, Denmark, 2005, pp. 1–13.
[25] T. Horyna, C.E. Venture, Summary of HCT building ambient vibration data analyses, Proceedings of the 18th International Modal Analysis Conference, Society for Experimental Mechanics (SEM), San Antonio, TX, USA, 2000, pp. 1095-1098.
[26] Y. Tamura, L. Zhang, A. Yoshida, K. Cho, S. Nakata, S. Naito, Ambient vibration testing and modal identification of an office building, Proceedings of the 20th International Modal Analysis Conference, Society for Experimental Mechanics (SEM), Los Angeles, CA, USA, 2002, pp. 141-146.
[27] T. Nagayama, S.H. Sim, Y. Miyamori, B.F. Spencer, Issues in structural health monitoring employing smart sensors, Smart Structures and Systems, 3 (2007) 299-320.
[28] T. Nguyen, T.H.T. Chan, D.P. Thambiratnam, Controlled Monte Carlo data generation for statistical damage identification employing Mahalanobis squared distance, Structural Health Monitoring, 13 (2014) 461-472.
[29] T. Nguyen, T.H.T. Chan, D.P. Thambiratnam, Field validation of controlled Monte Carlo data generation for statistical damage identification employing Mahalanobis squared distance, Structural Health Monitoring, 13 (2014) 473-488.